# Impacts of Clinker Storages Heat Transfer, Its Effect on Vertical Roller Cement Performances: A Case Study of Cement Grinding Operations in Nigeria.


## ABSTRACT

Practical and operation data indicates that vertical roller cement mills (VRCM) consumed low energy when compared to horizontal/ball mills. A case study of a vertical roller cement mills was carried out in Nigeria which was experiencing a lower production output and a higher energy consumption. This research was to investigate reasons behind the low production output on the VRCM. A thorough analysis was carried on the clinker storage facilities and the heat transfer across the composite cylindrical clinker silo walls (off – spec and main clinker) both silos having the same design but different dimensions and with different application purpose. The off-spec clinker silo has a design capacity of 1,800 tons and main clinker silo a design capacity of 60, 000 tons and both silo stores hot clinker that left the kiln clinker cooler at approximate temperature of 95$^{o}$C. The analytical results shows that the rate of heat transfer across the main clinker composite walls was 728 kW and the rate of heat transfer across the off-spec clinker composite walls was 217.15 kW. Numerical simulation was carried out using ANSYS simulation package and the results obtained were in good agreement with the results obtained theoretically. The ratio of heat loss on the main clinker composite walls to off-spec clinker composite walls was 3.35:1.



**Keywords:** Heat Transfer, Composite Cylindrical Walls, Vertical Roller Cement Mills, Clinker Silos, Cement Grinding, and Cement Temperature


## 1.0 INTRODUCTION

Cement grinding operation is the final stage cement production process in cement manufacturing. Ordinary Portland Cement (OPC) is the most common type of cement produced around the world when compared with other type of cement produced [1]. European standard further elaborated the most common type cements produced. However, some special cements are produced for a specific purpose such as low-heat cements or low-alkali cements as standardized by European standard EN 197-1. The European standard EN 197-1 and America standard (ASTM); described 27 types of cements, which were further divided into five (5) groups, as shown in Table 1, [2-7]. There are several types of cement grinding mills that are used in cement manufacturing plants. Table 2, are the list of cement grinding mills and it grinding efficiency, [8-10].

Table 1: Type of Cement Industry.

| | Types of Cement | Clinker % | Other Constituents |
|---|---|---|---|
| CEM I | Portland | 95-100 | |
| CEM II | Portland-slag | 65-94 | Blast furnace slag |
| | Portland-silica fume | 90-94 | Silica fume |
| | Portland-pozzolana | 65-94 | Pozzolana |
| | Portland-fly ash | 65-94 | Fly ashes |
| | Portland-burnt shale | 65-94 | Burnt Shale's |
| | Portland-limestone | 65-94 | Limestone |
| | Portland-composite | 65-94 | Additives mix |
| CEM III | Blast furnace | 5-64 | Additives mix |
| CEM IV | Pozzolanic | 45-89 | Additives mix |
| CEM V | Composite | 20-64 | Additives mix |

Table 2 Common Grinding Mills in the Cement

| Grinding Equipment | Grinding Force | Energy Use kWh/t(cement) | Grinding Efficiency |
|---|---|---|---|
| Tube Mill | Impact/Friction | 35-38 | 5-8% |
| Roller Press | Compression/Friction | 22-26 | 12-20% |
| Vertical Roller Mill | Compression/Friction | 27-30 | 7-15% |
| Horizontal Roller Mill | Compression/ Friction | 24-27 | 10-18% |

There are two major types of equipment used for cement grinding namely: Horizontal Ball Mill (HBM) and Vertical Roller Cement Mill (VRCM). The horizontal mills also known as ball mills has two (2) chamber which are separated by a diaphragms. The first chamber contains grinding media sizes between 60 mm to 90 mm. The grinding media are mostly made up of alloy- steel. While chamber two (2) contains grinding media sizes ranges between 50 mm to 15 mm. Figure 1 and Figure 2, shows the general overview of the horizontal or balls and vertical roller cement mill, [11,12].

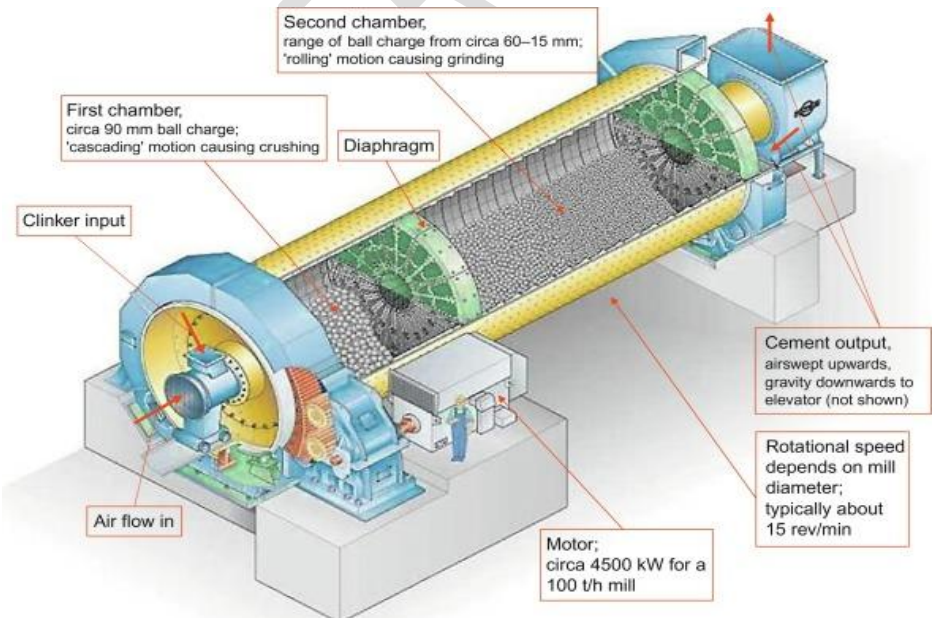

Figure 1. Overview of Horizontal or Ball Mill

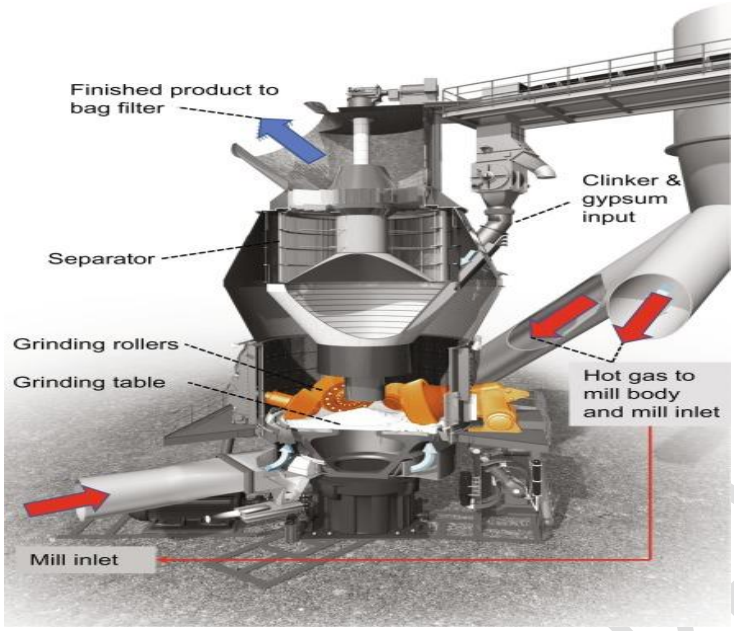


Figure 2. Overview of Vertical Roller Cement Mill VRCM

This research will be focusing more on optimizing vertical roller cement mills and the impacts of heat transfers/heat losses that are associated with vertical roller cement mills production output. Figure 3, shows the clinker main silo and off-spec clinker silo [13,14].

This research dated in 22nd December, 2021 and completed 21st December,2022 in a Nigeria Cement Plant (OPC).


Figure 3: An image of a Main clinker silo and Off – Spec silo in an existing cement plant

## 2. MATERIALS AND METHODOLOGY

A vertical roller cement mills was used for purpose of carrying out this research. Some of the data used are direct input and output of the running plant based on design of equipment supplied by the manufacture and it operating parameters.

The vertical roller cement mill has a design capacity 170 tons per hour with an additional hot gas generator for generating heat whenever vertical roller cement mills are in operation at temperature of 320 $^{o}$C.

**Heat generation (input and output) in cement grinding**

Production of OPC, it is assumed that the heat input consists of the grinding heat $Q_g$ and the heat in clinker $Q_{clk}$ as expressed in Equations (1) and (3) respectively, [15]. Cement grinding heat $Q_g$ is a direct function of the installed motor power (N) where the clinker heat depends directly on its temperature, [15],

$$Q_g = \frac{3.6\eta N}{G} \quad (1)$$

Clinker heat generation:

$$Q_{PK} = C_{PK}(T_{clk} - T_o) \quad (2)$$

$$C_{PK} = (0.00046T_{clk} + 0.733) \quad (3)$$

where; $N$ is motor power (kW) of mill, $\eta$ is mill drive efficiency (%), $cp_k$ is specific heat value for clinker (kJ/kg $^{o}$C), $T_{clk}$ is clinker outlet temperature ($^{o}$C), $G$ is mill output (t/h), $T_o$ is ambient air temperature ($^{o}$C). The heat loss with cement grinding outlet temperature is shown in Equations (4) and (5).

$$Q_C = C_{PC}(T_{cem} - T_o) \quad (4)$$

$$C_{PC} = (0.00046T_{cem} + 0.733) \quad (5)$$

where, $c_{Pc}$ is specific heat capacity for cement (kJ/kg $^{o}$C), $T_{cem}$ is cement temperature ($^{o}$C).

Heat losses due to radiation and convection which is the function of the surface of the mill and mill shell temperature is expressed in Equation (6).

$$Q_{r/C} = \frac{D_o \pi k (D_d/2 + L_l)}{1000\, G} \quad (6)$$

where, $D_d$ is nominal mill diameter (m), $D_o$ is the mill outer diameter (m), $L_l$ *is* mill length (m), $k$ is heat transfer factor (kJ/m$^2$h). The heat transfer factors (k) for clinker grinding heat varies with some parameters like the diameter of the mill, [8].

For an open circuit mills k is (4000 kJ/m$^2$h) for diameter greater than 2 meters but less than 3.5 meters. For close circuit cement mill with diameter less than 3.5 m, k is 8000 kJ/m$^2$h, close circuit cement mill with diameter greater than 3.5 m, k is 12000 kJ/m$^2$h, [15].

Heat output due to venting air, is expressed in Equation (7):

$$Q_g = \left[(Q_g + Q_c) - (Q_c + Q_{r/c} + Q_w)\right] \quad (7)$$

The heat output due to water evaporation, is expressed in Equation (8):

$$Q_w = \frac{rw}{1000} \quad (8)$$

where; *w* is water rate (including moisture content in feed material) (kg/t) *r* is heat of evaporation of the water and has the value of 2500 kJ/kg. Heat generation output consists of the heat contained in the cement ($Q_c$), the heat lost by radiation and convection ($Q_{r/c}$), the heat removed by air ($Q_a$) and by evaporation of water ($Q_w$). Heat contained in cement depends only on the cement outlet temperature, [15]. Venting air volume ($V_{air}$) is dependent on the energy balance resulting from heat input and input during cement powder production. It is expressed in equation (9a), [15].

$$V_{air} = \frac{1000 \times G \times Q_a}{c_{pair}\,(t_{air} - t_o)} (Nm^3/h) \quad (9a)$$

The required water injection W is determined using Equation (9b),

$$W = \frac{1000 \times Q_a}{r} \quad (9b)$$

**Heat Transfers across the Composite Cylindrical Clinker Silo Walls**

The following basic assumptions were used for the research:

- the concrete silo is homogeneous and isotropic;
- there is no internal heat generation;
- contact between clinker and silo wall is sufficient for conduction to occur;
- heat transfer resistance is negligible;
- heat transfer by convection and radiation is negligible; and
- conduction occurs at steady state.

Figure 4a to Figure 4b, shows the third (3rd ) angle projection of composite cylindrical (main and off-spec) silos used for the storing of the clinker that is used by the vertical roller cement mills for cement grinding operation and the dimensions of the silos. Clinker temperature insider the silos is 95 $^{o}$C.

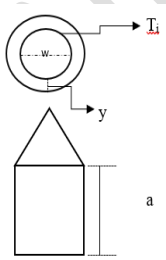


Figure 4a. The main clinker silo

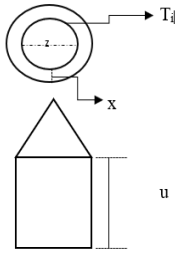


Figure 4b. The off-spec silo

Outer clinker silo wall temperature or ambient temperature ($T_o$) and ($T_i$) is the inner silo wall temperature or clinker temperature silo. Table 3, contains information about the main and off-spec clinker silo design parameter and design capacity for the vertical roller cement mills that was used for this research in Nigeria.

Table 3: Geometrical and operational parameters

| Parameter | Main Clinker Silo | Off-Spec Clinker Silo | Unit |
|---|---|---|---|
| Thickness | 0.75 | 0.50 | m |
| Diameter | 44.50 | 10.50 | m |
| Inner radius | 22.25 | 5.25 | m |
| Outer radius | 23 | 5.75 | m |
| Height | 20 m | 16.40 | m |
| Design Capacity | 60,000 (60,000,000) | 1,800 (1,8000,000) | Tons (kg) |
| Clinker temperature inside silo | 95 (368) | 95 (368) | $^{o}$C (K) |
| Ambient temperature | 35 (308) | 35 (308) | $^{o}$C (K) |
| Heat loss across wall | 728 | 217.51 | kW |

**Heat Transfer across Walls Analysis**

Basic requirements for heat transfer is the presence of a temperature differences. Analyzing the heat transfer across cylindrical coordinates of a solid walls (main clinker silo and off-spec silo) with infinitesimal thickness δr and height L, with an assumption that temperature is radially symmetric and across a volume (V), as shown in Figure 4c, [16-19].

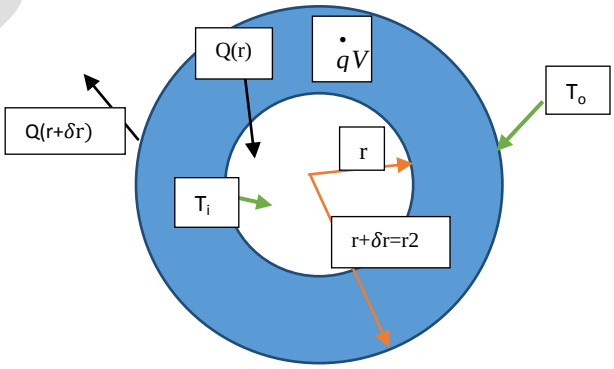


Figure 4c. Heat Transfer across Sliced Solid Wall.

The possibility of internal energy generation ( $\dot{q}$ ) due to hot clinker that are been stored insider the cylindrical composite silo. Heat Q(r) flows *in* from the left, and Q(r+δr) flows *out* through the right. The energy balance is show in equation (10a) and (10b)

$$Q_{in} - Q_{out} = mc\left(\frac{\partial T}{\partial t}\right) \tag{10a}$$

$$Q(r) + \dot{q} - Q(r+\delta r) = mc\left(\frac{\partial T}{\partial t}\right)$$

(10b)

$$V = \pi(r+\delta r)^2 L - \pi r^2 L \approx 2\pi r \delta r L \tag{10c}$$

Dropping $(\delta r)^2$ terms because $\delta r << r$, $m$ is the mass flow, $c$ is the specific heat

Quantities of heat rate (Q) flowing through a solid with cross-sectional area *A*, this is expressed in equation (11) to (12d) [16-19].

$$Q = qA \tag{11}$$

$$q = (-k\frac{\partial T}{\partial r})A \tag{12a}$$

$$A = 2\pi dr \tag{12b}$$

$$\int_{r}^{r+\delta r} \frac{Q}{A}\partial r = -\int_{T1}^{T2} k\partial T \tag{12c}$$

$$Q = 2\pi Lk\frac{T_i - T_o}{In\frac{r_2}{r}} \tag{12d}$$

where $q$ is steady heat flux, substituting into equation (10b), substituting equation (10c), equation (11) and (12) into equation (10b) gives equation (13)

$$-k2\pi rL\frac{\partial T}{\partial r}\Big|_r + \dot{q}\,2\pi r\delta rL + k2\pi(r+\delta r)L\,\frac{\partial T}{\partial r}\Big|_{r+\delta r} = mc\frac{\partial T}{\partial t} \tag{13}$$

For linear functions as expressed in equation (14) and (15)

$$f(x+dx) = f(x) + f^{l}(x)dx \tag{14}$$

$$f^{l}(x+\delta x) = f^{l}(x) + f^{ll}(x)dx \tag{15}$$

Using linear function gives equation (16)

$$\frac{\partial T}{\partial r}\Big|_{r+\delta r} \approx \left(\frac{\partial T}{\partial r}\right)\Big|_{r} + \frac{\partial^2 T}{\partial r^2}\delta r \tag{16}$$

Substituting equation (16) into (13)

$$2\pi kL\left(r\delta r\frac{\partial^2 T}{\partial r^2} + \delta r\frac{\partial T}{\partial r}\right) + \dot{q}\,2\pi r\delta rL = mc\frac{\partial T}{\partial t} \tag{17}$$

$m = \rho 2\pi r\delta rL$, and $\alpha = \dfrac{k}{\rho c}$ Thermal diffusivity substituting into equation (17)

$$\frac{\partial^2 T}{\partial r^2} + \frac{1}{r}\frac{\partial T}{\partial r} + \frac{\dot{q}}{k} = \frac{1}{\alpha}\frac{\partial T}{\partial t} \tag{18}$$

Heat equation for cylindrical coordinates across the clinker silo walls is expressed (19)

$$\frac{1}{r}\frac{\partial}{\partial r}\left(r^2\frac{\partial T}{\partial r}\right) + \frac{\dot{q}}{k} = \frac{1}{\alpha}\frac{\partial T}{\partial t} \tag{19}$$

**Validation of the of Theoretical Results with Numerical Results (ANSYS)**

In order to further investigate the heat loss across the Composite Cylindrical Clinker Silo Walls for the Off- Spec Clinker Silo and the Composite Cylindrical Clinker Silo Walls for the Main Clinker Silo, thermal analysis was carried out in ANSYS – Mechanical platform. A 3D cylindrical geometries of the main silo and off-spec silo were developed in SolidWork platform and it was imported in ANSYS – Mechanical thermal analysis platform.

**Meshing:** The 3-D models as shown in Figures 5 and 6 shows cylindrical geometry for the main silo and off – spec silo respectively and these were meshed into ANSYS meshing environment, where the model were discretized into finite element mesh. The number of elements in a mesh were varied, depending on the level of refinement or size of the cells in the mesh and hence a very fine mesh size was used, taking into consideration computation time and solution accuracy. Figure 7 and 8, shows the meshing results for both main clinker silo and off-spec clinker silo.

**Boundary Conditions:** For the silos (the main silo and off-spec silo), the inner temperature of the wall of the silo is assigned to be 95℃ while the wall temperature of the outer surface of the silo is assigned 35℃., as shown in Figures 9

and 10 respectively. Every other surface is assumed to be adiabatic (No heat loss) surface, a steady – state thermal analysis is carried out or computed by the solver.

**Solution Results:** The primary target in this research is the estimation of heat transfer rate across the wall of the silo and this was expressed in equation (12d). The heat transfer rate has been estimated theoretically, and the results presented. The simulation results on other hand enables the estimation of heat flux as shown in Figure 11 and 12. Similarly from equation (12d), is can be seen that heat transfer rate is given by the product of heat flux and cross sectional area. Hence the value of heat flux estimated from the simulation is provided for both main silo and the off-spec silo, shown in Tables 10 to 13.

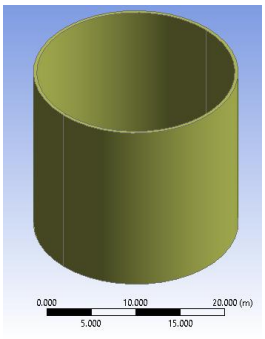


Figure 5: 3D model of main silo

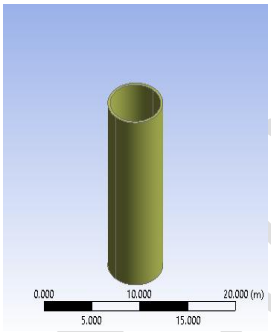


Figure 6: 3D model of off – spec silo

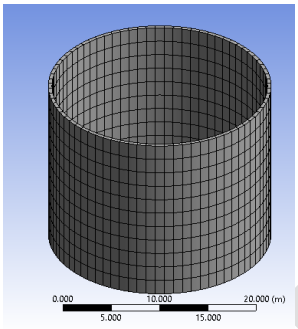


Figure 7: Mesh of main silo

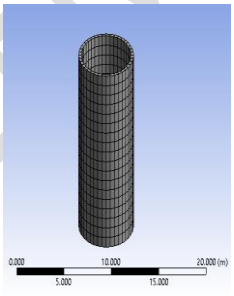


Figure 8: Mesh of off – spec silo

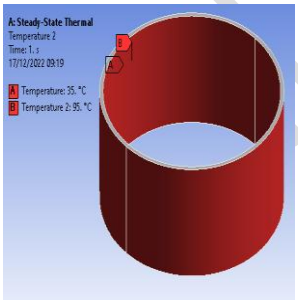


Figure 9: Boundary Condition on main silo

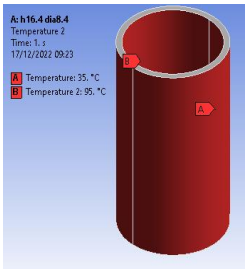


Figure 10: Mesh of off – spec silo

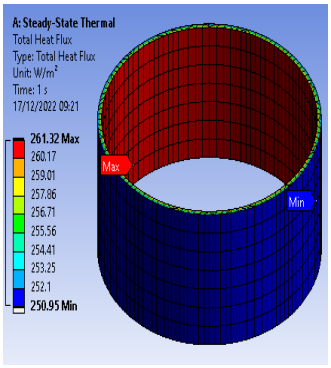


Figure 11: Heat flux on of main silo wall

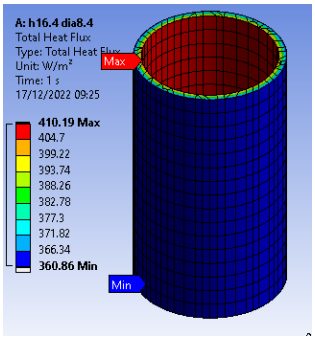


Figure 12: Heat flux on off - spec silo wall

## 3.0 RESULTS and DISCUSSIONS

### Theoretical Results

The results obtained from the analysis of heat loss across the composite cylindrical clinker silo walls for the off- spec clinker silo and heat loss across the composite cylindrical clinker silo walls for the main clinker silo are presented. The rate of heat transfer/loss across composite cylindrical clinker for the two silos is shown on Figure 13, temperature gradient.

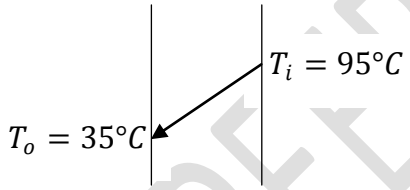


Figure 13: Temperature gradient from $T_i$ (inner wall temperature) to $T_o$ (outer wall temperature)

Table 4, shows the analysis on impact of 10% reduction on main clinker silo height against heat loss across the wall, keeping other parameter constant. Table 5, shows the analysis on impact of 10% reduction on the main clinker silo inner radial against heat loss across the wall of the main clinker silo, keeping other parameter constant.

| $a$ $(m)$ | $k$ $(W/mK)$ | $W$ $(m)$ | $T_i$ $(K)$ | $T_o$ $(K)$ | $y\ (m)$ | $r_i\ (m)$ | $r_o\ (m)$ | $Q_{ms}$ $(KW)$ |
|---|---|---|---|---|---|---|---|---|
| **20** | 3.2 | 44.5 | 368 | 308 | 0.75 | 22.250 | 23.000 | 727.87 |
| **20** | 3.2 | 40.05 | 368 | 308 | 0.75 | 20.025 | 20.775 | 656.28 |
| **20** | 3.2 | 35.6 | 368 | 308 | 0.75 | 17.800 | 18.550 | 584.68 |
| **20** | 3.2 | 31.15 | 368 | 308 | 0.75 | 15.575 | 16.325 | 513.08 |
| **20** | 3.2 | 26.7 | 368 | 308 | 0.75 | 13.350 | 14.100 | 441.48 |
| **20** | 3.2 | 22.25 | 368 | 308 | 0.75 | 11.125 | 11.875 | 369.87 |
| **20** | 3.2 | 17.8 | 368 | 308 | 0.75 | 8.900 | 9.650 | 298.25 |

Table 4: Main clinker height *against* heat loss (10%)

| *a* (m) | *k* (W/mK) | *W (m)* | $T_i$ (K) | $T_o$ (K) | *y* (m) | $Q_{ms}$ (kW) |
|---|---|---|---|---|---|---|
| 20 | 3.2 | 44.5 | 368 | 308 | 0.75 | 727.87 |
| 18 | 3.2 | 44.5 | 368 | 308 | 0.75 | 655.08 |
| 16 | 3.2 | 44.5 | 368 | 308 | 0.75 | 582.30 |
| 14 | 3.2 | 44.5 | 368 | 308 | 0.75 | 509.51 |
| 12 | 3.2 | 44.5 | 368 | 308 | 0.75 | 436.72 |
| 10 | 3.2 | 44.5 | 368 | 308 | 0.75 | 363.94 |
| 8 | 3.2 | 44.5 | 368 | 308 | 0.75 | 291.15 |
| 6 | 3.2 | 44.5 | 368 | 308 | 0.75 | 218.36 |
| 4 | 3.2 | 44.5 | 368 | 308 | 0.75 | 145.57 |
| 2 | 3.2 | 44.5 | 368 | 308 | 0.75 | 72.79 |

| *a (m)* | *k (W/mK)* | *z (m)* | $T_i$ (K) | $T_o$ (K) | *x (m)* | $Q_{os}$ (kW) |
|---|---|---|---|---|---|---|
| 16.40 | 3.2 | 10.5 | 368 | 308 | 0.5 | 217.51 |
| 14.76 | 3.2 | 10.5 | 368 | 308 | 0.5 | 195.76 |
| 13.12 | 3.2 | 10.5 | 368 | 308 | 0.5 | 174.01 |
| 11.48 | 3.2 | 10.5 | 368 | 308 | 0.5 | 152.26 |
| 9.84 | 3.2 | 10.5 | 368 | 308 | 0.5 | 130.50 |
| 8.20 | 3.2 | 10.5 | 368 | 308 | 0.5 | 108.75 |
| 6.56 | 3.2 | 10.5 | 368 | 308 | 0.5 | 87.00 |
| 4.92 | 3.2 | 10.5 | 368 | 308 | 0.5 | 65.25 |
| 3.28 | 3.2 | 10.5 | 368 | 308 | 0.5 | 43.50 |
| 1.64 | 3.2 | 10.5 | 368 | 308 | 0.5 | 21.75 |

7: off-spec clinker silo radial against heat loss

| | | | | | | | | |
|---|---|---|---|---|---|---|---|---|
| **20** | 3.2 | 13.35 | 368 | 308 | 0.75 | 6.675 | 7.425 | 226.61 |
| **20** | 3.2 | 8.9 | 368 | 308 | 0.75 | 4.450 | 5.200 | 154.93 |
| **20** | 3.2 | 4.45 | 368 | 308 | 0.75 | 2.225 | 2.975 | 83.07 |

Table 5: Main clinker silo inner radial against heat loss (10%)

Table 6, shows the analysis on impact of 10% reduction on off- spec clinker silo height against heat loss across the wall, keeping other parameter constant. Table 7, shows the analysis on impact of 10% reduction on off- spec clinker silo radial ($r_i$) against heat loss ($Q_{os}$)across the wall, keeping other parameter constant.

Table 6: Off-spec clinker silo against heat transfer Table

| *u* (m) | *k* (W/mK) | *z (m)* | $T_i$ (K) | $T_o$ (K) | *x* (m) | $r_i$ (m) | $r_o$ (m) | $Q_{os}$ (KW) |
|---|---|---|---|---|---|---|---|---|
| 16.4 | 3.2 | 10.50 | 368 | 308 | 0.5 | 5.250 | 5.750 | 217.51 |
| 16.4 | 3.2 | 9.45 | 368 | 308 | 0.5 | 4.725 | 5.225 | 196.72 |
| 16.4 | 3.2 | 8.40 | 368 | 308 | 0.5 | 4.200 | 4.700 | 175.92 |
| 16.4 | 3.2 | 7.35 | 368 | 308 | 0.5 | 3.675 | 4.175 | 155.12 |
| 16.4 | 3.2 | 6.30 | 368 | 308 | 0.5 | 3.150 | 3.650 | 134.31 |
| 16.4 | 3.2 | 5.25 | 368 | 308 | 0.5 | 2.625 | 3.125 | 113.49 |
| 16.4 | 3.2 | 4.20 | 368 | 308 | 0.5 | 2.100 | 2.600 | 92.65 |
| 16.4 | 3.2 | 3.15 | 368 | 308 | 0.5 | 1.575 | 2.075 | 71.77 |
| 16.4 | 3.2 | 2.10 | 368 | 308 | 0.5 | 1.050 | 1.550 | 50.81 |
| 16.4 | 3.2 | 1.05 | 368 | 308 | 0.5 | 0.525 | 1.025 | 29.57 |

Table 8, shows production log-sheet of a vertical roller cement mill of a running plant in Nigeria with low production output (134 tph) while using the main clinker silo with capacity of 60,000 tons using hot gas generator, dated: 3rd March, 2022 and Table 8, shows production log-sheet of a vertical roller cement mill of a running plant in Nigeria with improved cement production (150 tph) while using off-spec clinker silo capacity (1,800 tons) without using hot gas generator dated: 10th October, 2022.

Table 8: Low Production Output Using Main Clinker silo (3rd March, 2022)

| **Time** | **Clinker** | **Limestone** | **Gypsum** | **Feed Rate** | **Hot Gas Generator** | **Mill Inlet Temperature** | **Mill Outlet Temperature** |
|---|---|---|---|---|---|---|---|
| | **Tons** | **Tons** | **Tons** | **TPH** | **($T_{HGG}$) $^{o}$C** | **$^{O}$C** | **$^{O}$C** |
| 07:00 | 116.375 | 13.3 | 3.325 | 133 | 335 | 101 | 92 |
| 08:00 | 116.375 | 13.3 | 3.325 | 133 | 330 | 101 | 92 |

| | | | | | | | |
|---|---|---|---|---|---|---|---|
| 09:00 | 117.25 | 13.4 | 3.35 | 134 | 332 | 100 | 92 |
| 10:00 | 117.25 | 13.4 | 3.35 | 134 | 338 | 100 | 92 |
| 11:00 | 117.25 | 13.4 | 3.35 | 134 | 337 | 100 | 92 |
| 12:00 | 117.25 | 13.4 | 3.35 | 134 | 334 | 100 | 91 |
| 13:00 | 117.25 | 13.4 | 3.35 | 134 | 335 | 100 | 91 |
| 14:00 | 117.25 | 13.4 | 3.35 | 134 | 339 | 100 | 91 |
| 15:00 | 117.25 | 13.4 | 3.35 | 134 | 342 | 100 | 91 |
| 16:00 | 117.25 | 13.4 | 3.35 | 134 | 328 | 100 | 91 |
| 17:00 | 117.25 | 13.4 | 3.35 | 134 | 332 | 100 | 91 |
| 18:00 | 117.25 | 13.4 | 3.35 | 134 | 337 | 100 | 91 |
| 19:00 | 117.25 | 13.4 | 3.35 | 134 | 341 | 100 | 91 |
| 20:00 | 117.25 | 13.4 | 3.35 | 134 | 331 | 100 | 91 |
| 21:00 | 117.25 | 13.4 | 3.35 | 134 | 334 | 100 | 91 |
| 22:00 | 117.25 | 13.4 | 3.35 | 134 | 332 | 100 | 91 |
| 23:00 | 117.25 | 13.4 | 3.35 | 134 | 330 | 100 | 91 |
| 00:00 | 117.25 | 13.4 | 3.35 | 134 | 332 | 100 | 91 |
| 01:00 | 117.25 | 13.4 | 3.35 | 134 | 338 | 100 | 91 |
| 02:00 | 117.25 | 13.4 | 3.35 | 134 | 331 | 100 | 91 |

Table 9: Improve Production Output Using Off-spec Clinker silo (10th October, 2022)

| **Time** | Clinker | Limestone | Gypsum | Total Feed Rate | Hot Gas Generator | Temperature Mill Inlet | Mill Outlet |
|---|---|---|---|---|---|---|---|
| | **Tons** | **Tons** | **Tons** | **Tons Per Hour** | **($T_{HGG}$) $^{o}$C** | **$^{O}$C** | **$^{O}$C** |
| 7:00 | 130.5 | 15 | 4.5 | 150 | Not in use | 101 | 93 |
| 8:00 | 130.5 | 15 | 4.5 | 150 | Not in use | 101 | 93 |
| 9:00 | 130.5 | 15 | 4.5 | 150 | Not in use | 99 | 94 |
| 10:00 | 130.5 | 15 | 4.5 | 150 | Not in use | 99 | 94 |
| 11:00 | 130.5 | 15 | 4.5 | 150 | Not in use | 99 | 94 |
| 12:00 | 130.5 | 15 | 4.5 | 150 | Not in use | 99 | 94 |
| 13:00 | 130.5 | 15 | 4.5 | 150 | Not in use | 99 | 93 |
| 14:00 | 130.5 | 15 | 4.5 | 150 | Not in use | 99 | 93 |
| 15:00 | 130.5 | 15 | 4.5 | 150 | Not in use | 99 | 93 |
| 16:00 | 130.5 | 15 | 4.5 | 150 | Not in use | 99 | 93 |
| 17:00 | 130.5 | 15 | 4.5 | 150 | Not in use | 99 | 93 |
| 18:00 | 130.5 | 15 | 4.5 | 150 | Not in use | 99 | 93 |
| 19:00 | 130.5 | 15 | 4.5 | 150 | Not in use | 99 | 93 |
| 20:00 | 130.5 | 15 | 4.5 | 150 | Not in use | 99 | 93 |
| 21:00 | 130.5 | 15 | 4.5 | 150 | Not in use | 99 | 93 |
| 22:00 | 130.5 | 15 | 4.5 | 150 | Not in use | 99 | 93 |

| | | | | | | | |
|---|---|---|---|---|---|---|---|
| 23:00 | 130.5 | 15 | 4.5 | 150 | Not in use | 99 | 93 |
| 00:00 | 130.5 | 15 | 4.5 | 150 | Not in use | 99 | 93 |
| 01:00 | 130.5 | 15 | 4.5 | 150 | Not in use | 99 | 93 |
| 02:00 | 130.5 | 15 | 4.5 | 150 | Not in use | 99 | 94 |

Table 8 and Table 9 are direct physical log-sheets of a running vertical roller cement mill plant in Nigeria. Table 7, shows the impacts of heat loss across the composite walls of the main clinker with vertical roller cement mill production output of 134 tons per hour and continuous running of hot gas generator. While Table 9, using off-spec composite clinker silo shows the impact of reduction in heat loss on the vertical roller cement performance with production output of 150 tons per hour and a zero (0) use of the hot gas generator.

**Results Validation Using ANSYS**

The result obtained from the simulation is basically the maximum, minimum and average heat flux estimated for each configuration of silo. For each type of silo and the dimensions, the theoretical values of heat transfer rate and heat flux are shown. These results are shown in tables 10 to 13.

Table 10: Impact of 10% reduction main clinker height against heat loss ($Q_{ms}$) across the main clinker silo using Ansys simulation

| *a (m)* | *W (m)* | *y (m)* | $\boldsymbol{Q_{ms}}$ *(kW)* | *q* theory | *q Ansys* | | |
|---|---|---|---|---|---|---|---|
| | | | | | Max | Min | Avg |
| 20 | 44.5 | 0.75 | 727.87 | 256 | 260.83 | 251.23 | 256.24 |
| 18 | 44.5 | 0.75 | 655.08 | 256 | 260.82 | 251.56 | 255.96 |
| 16 | 44.5 | 0.75 | 582.30 | 256 | 260.82 | 251.57 | 255.96 |
| 14 | 44.5 | 0.75 | 509.51 | 256 | 260.31 | 251.66 | 256.02 |
| 12 | 44.5 | 0.75 | 436.72 | 256 | 260.83 | 251.23 | 256.24 |
| 10 | 44.5 | 0.75 | 363.94 | 256 | 260.82 | 251.56 | 255.96 |
| 8 | 44.5 | 0.75 | 291.15 | 256 | 260.82 | 251.57 | 255.96 |
| 6 | 44.5 | 0.75 | 218.36 | 256 | 260.31 | 251.66 | 256.02 |
| 4 | 44.5 | 0.75 | 145.57 | 256 | 260.82 | 251.57 | 255.96 |
| 2 | 44.5 | 0.75 | 72.79 | 256 | 260.31 | 251.66 | 256.02 |

Table 11: Impact of 10% reduction on the main clinker silo inner radial ($r_i$) against heat loss ($Q_{ms}$)across the main clinker silo Ansys simulation

| *a (m)* | *W (m)* | *y (m)* | $r_i$ *(m)* | $r_o$ *(m)* | $Q_{ms}$ *(KW)* | *q* theory | *q CFD* | | |
|---|---|---|---|---|---|---|---|---|---|
| | | | | | | | Max | Min | Avg |
| 20 | 44.5 | 0.75 | 22.250 | 23.000 | 727.87 | 256 | 260.83 | 251.23 | 256.24 |
| 20 | 40.05 | 0.75 | 20.025 | 20.775 | 656.28 | 256 | 261.32 | 250.95 | 256.11 |
| 20 | 35.6 | 0.75 | 17.800 | 18.550 | 584.68 | 256 | 261.95 | 250.41 | 255.69 |

| | | | | | | | | | |
|---|---|---|---|---|---|---|---|---|---|
| 20 | 31.15 | 0.75 | 15.575 | 16.325 | 513.08 | 256 | 262.76 | 249.76 | 256.19 |
| 20 | 26.7 | 0.75 | 13.350 | 14.100 | 441.48 | 256 | 263.18 | 248.81 | 256.03 |
| 20 | 22.25 | 0.75 | 11.125 | 11.875 | 369.87 | 256 | 265.03 | 247.42 | 256.1 |
| 20 | 17.8 | 0.75 | 8.900 | 9.650 | 298.25 | 256 | 267.87 | 245.34 | 255.54 |
| 20 | 13.35 | 0.75 | 6.675 | 7.425 | 226.61 | 256 | 271.71 | 241.87 | 257.21 |
| 20 | 8.9 | 0.75 | 4.450 | 5.200 | 154.93 | 256 | 280 | 235.13 | 256.95 |
| 20 | 4.45 | 0.75 | 2.225 | 2.975 | 83.07 | 256 | 298.11 | 218.87 | 259.54 |

Table 12: Impact of 10% height reduction on off-spec clinker silo against heat transfer across the off-spec clinker silo wall Ansys simulation

| *u (m)* | *z (m)* | *x (m)* | $Q_{os}$ *( (kW)* | *q* theory | *q Ansys* | | |
|---|---|---|---|---|---|---|---|
| | | | | | Max | Min | Avg |
| 16.4 | 10.5 | 0.5 | 217.51 | 384 | 402.44 | 365.8 | 384.13 |
| 14.76 | 10.5 | 0.5 | 195.76 | 384 | 402.44 | 365.8 | 384.13 |
| 13.12 | 10.5 | 0.5 | 174.01 | 384 | 402.44 | 365.8 | 384.13 |
| 11.48 | 10.5 | 0.5 | 152.26 | 384 | 402.44 | 365.8 | 384.13 |
| 9.84 | 10.5 | 0.5 | 130.50 | 384 | 402.44 | 365.8 | 384.13 |
| 8.2 | 10.5 | 0.5 | 108.75 | 384 | 402.44 | 365.8 | 384.13 |
| 6.56 | 10.5 | 0.5 | 87.00 | 384 | 402.44 | 365.8 | 384.13 |
| 4.92 | 10.5 | 0.5 | 65.25 | 384 | 402.44 | 365.8 | 384.13 |
| 3.28 | 10.5 | 0.5 | 43.50 | 384 | 402.44 | 365.8 | 384.13 |
| 1.64 | 10.5 | 0.5 | 21.75 | 384 | 402.44 | 365.8 | 384.13 |

Table 13: Impact of 10% reduction on off-spec clinker silo radial ($r_i$) against heat loss ($Q_{os}$) across the wall of off-spec clinker silo ANSYS simulation

| *a (m)* | *W (m)* | *y (m)* | $r_i$ *(m)* | $r_o$ *(m)* | $Q_{ms}$ *(KW)* | *q* theory | *q Ansys* | | |
|---|---|---|---|---|---|---|---|---|---|
| | | | | | | | Max | Min | Avg |
| 16.4 | 10.5 | 0.5 | 5.250 | 5.750 | 217.51 | 384 | 402.44 | 365.8 | 384.13 |
| 16.4 | 9.45 | 0.5 | 4.725 | 5.225 | 196.72 | 384 | 405.69 | 363.76 | 385.64 |
| 16.4 | 8.4 | 0.5 | 4.200 | 4.700 | 175.92 | 384 | 410.19 | 360.86 | 382.98 |
| 16.4 | 7.35 | 0.5 | 3.675 | 4.175 | 155.12 | 384 | 415.86 | 357.5 | 383.99 |
| 16.4 | 6.3 | 0.5 | 3.150 | 3.650 | 134.31 | 384 | 422.61 | 353.13 | 381.86 |
| 16.4 | 5.25 | 0.5 | 2.625 | 3.125 | 113.49 | 384 | 422.03 | 349.47 | 382.62 |
| 16.4 | 4.2 | 0.5 | 2.100 | 2.600 | 92.65 | 384 | 433.52 | 340.03 | 389.95 |
| 16.4 | 3.15 | 0.5 | 1.575 | 2.075 | 71.77 | 384 | 446.85 | 330.54 | 391.39 |
| 16.4 | 2.1 | 0.5 | 1.050 | 1.550 | 50.81 | 384 | 470.61 | 312.86 | 387.93 |
| 16.4 | 1.05 | 0.5 | 0.525 | 1.025 | 29.57 | 384 | 548.4 | 275.8 | 385.76 |

**Comparison of Theoretical and ANSYS Results**

The results from theoretical and simulation analysis for main clinker silo with other dimensions and boundary condition were kept constant while 10% reduction on the height of the silo was investigated from 20 m to 2 m is presented as shown on Table 10. The results revealed that there is negligible difference between theoretically estimated heat flux and the simulation estimated value of heat flux. This implies that there is an agreement between the two approaches or analysis. The heat transfer rate for the simulation is not estimated because, it will still result in the same value as the theoretical. These results establish the validation of the two results. Unlike the theoretical value of the heat flux which is based of fundamental principal that the average value of heat flux across the silo is estimated, the simulation further reveals the maximum and minimum values, where we have the maximum value greater than the average and the minimum value lower than the average value. Another scenario considered is the configuration whereby the height and wall thickness of the main silo is kept constant, while the inner diameter was varied by 10% reduction. In this case, the theoretical and simulation analysis revealed that their respective values of heat flux estimated also has negligible difference, however, only when the average value of the simulation analysis is considered. The results revealed that average value of heat flux remains constant with reduction in inner diameter, there is a continuous increase in the maximum value of heat flux followed by continuous decrease in the minimum value of heat flux as seen in Table 10. The location on the silo where the heat flux is maximum and minimum can be seen and/or shown using a temperature probe as seen in Figures 11 and 12. The results for the off-spec silo are shown Tables 11 and 12. The variation and changes used in the main silo were similar to the main silo. The major difference between the two silos are in their initial height and inner diameters. The major differences are their geometrical values and estimated values of heat transfer and heat flux.

**CONCLUSIONS**

The heat loss across the composite cylindrical clinker silos are of various values. The following were observed during the course the research:

- ✓ The off-spec clinker silo has heat loss ($Q_{os}$) across the wall was 217.15 kW and the quantities of heat loss across main clinker was 728 kW. The large quantities of heat loss on main clinker was because of the design capacity of the main clinker silo of 60,000 tons (60,000,000 kg).
- ✓ It was also observed that due to large quantities of heat loosed across the main clinker could also be responsible for the use of hot gas generator continuously whenever the vertical roller cement mill is in operation using.
- ✓ The off-spec clinker silo was observed to have a lesser quantities heat loss across it walls when compared to the main clinker silo with more production output on the vertical roller cement mill of 150 tons per hour.
- ✓ Numerical simulation was carried out using ANSYS simulation package and the results obtained were in good agreement with the results obtained theoretically.
- ✓ The simulation result also provide temperature contour to shows the distribution of the temperature and heat flux on the silos. This reveals specific points on the silos where maximum heat is lost.
- ✓ The information provided by the temperature contour, the heat loss across the storage “containing high temperature” walls can be analyzed properly. This will help in the performance of the equipment to use the stored materials.

**ABBREVIATION**

| Symbol | Meaning | Unit |
|---|---|---|
| a | Main Clinker Silo Height | m |
| A | Cross sectional Area | $m^2$ |
| $A_i$ | Silo Inner Wall Cross-Sectional Area | $m^2$ |
| $A_{lm}$ | Log-mean Cross-Sectional Area | $m^2$ |
| $A_o$ | Silo Outer Wall Cross-Sectional Area | $m^2$ |
| ASTM | American Society for Testing Materials | |
| CaO | Lime | - |
| CEM | Cement | - |
| $cp_{air}$ | Specific Heat Capacity of air | kJ/kg $^oC$ |
| $cp_c$ | Specific Heat Capacity of Cement | kJ/kg $^oC$ |
| $cp_k$ | Specific Heat Capacity of Clinker | kJ/kg $^oC$ |
| $D_d$ | Nominal Mill Diameter | m |
| $D_o$ | Mill Outer Diameter | m |
| dr | Thickness of Concrete Silo | m |
| ETSAP | European Technology System Analysis Programme | - |
| G | Mill Output | tons/hr |
| h | Height of Concrete Silo | m |
| IEA | International Energy Agency | - |
| K | Thermal Conductivity of Concrete | W/K m |
| K | Heat Transfer Factor | $kJ/m^2hr$ |
| L | Thickness of walls | m |
| $L_l$ | Mill Length | m |
| N | Motor Power | kW |
| OPC | Ordinary Portland Cement | - |
| Q | Rate of Heat Transfer | kW |
| Q | Steady heat flux | kW |
| $Q_a$ | Heat Removed by Air | kW |
| $Q_c$ | Heat in Cement | kW |
| $Q_{clk}$ | Heat in Clinker | kW |
| $Q_g$ | Grinding Heat | kW |
| $Q_{r/c}$ | Heat Lost by Radiation and convection | kW |

| | | |
|---|---|---|
| $Q_w$ | Heat Removed by Evaporation of Water | kW |
| r | Water Heat of Evaporation | kJ/kg |
| $r_i$ | Inner Radius of Cylindrical Silo | m |
| $r_o$ | Outer Radius of Cylindrical Silo | m |
| $SiO_2$ | Silica | - |
| $t_{air}$ | Air Final Temperature | $^oC$ |
| $T_{cem}$ | Cement Temperature | $^oC$ |
| $T_{clk}$ | Clinker Outlet Temperature | $^oC$ |
| $T_{HGG}$ | Hot Gas Generator Temperature | $^oC$ |
| $T_i$ | Silo Inner Temperature | $^oC$ |
| $T_o$ | Ambient Air Temperature | $^oC$ |
| $t_o$ | Air Initial Temperature | $^oC$ |
| $T_o$ | Silo Outer Temperature | $^oC$ |
| u | Off-Spec Clinker Silo Height | m |
| $V_{air}$ | Venting Air Volume | $Nm^3/hr$ |
| W | Required Water Injection | kg/hr |
| w | Water Rate | kg/hr |
| x | Off-Spec Clinker Silo Thickness | m |
| y | Main Clinker Silo Thickness | m |
| $\pi$ | Pi | - |
| $\eta$ | Mill Drive Efficiency | % |



**References**


[1] Joseph O; Akintunde M; Dahunsi O; Yaru S and Idowu E (2022). Effect of Clinker Bed Height on Clinker Cooling Process on Clinker Grate Coolers Used in Cement Plant. IOSR Journal of Engineering, 12(11): pp.25-37.

[2] American Society for Testing Materials - ASTM C688-14 (2018). Standard Specification for Functional Additions for Use in Hydraulic Cements International, West Conshohocken, Philadelphia USA, pp. 1-18

[3] American Society for Testing Materials - ASTM C1565-19 (2018). Standard Test Method for Determination of Pack-Set Index of Portland and Blended Hydraulic Cements International, West Conshohocken, Philadelphia USA, pp.1-10

[4] American Society for Testing Materials - ASTM C441/C441M-17 (2018). Standard Test Method for Effectiveness of Pozzolans or Ground Blast-Furnace Slag in Preventing Excessive Expansion of Concrete Due to the Alkali-Silica Reaction, International, West Conshohocken, Philadelphia USA., pp. 1-8

[5] IEA ETSAP International Energy Agency and Energy Technology Systems Analysis Programme, (2010). Technology Briefings 103, pp. 1 – 8.

[6] Frauke S; Ioanna K; Bianca M; Serge R and Luis D (2013). Best Available Techniques (BAT) Reference Document for the Production of Cement, Lime and Magnesium Oxide. Industrial Emissions Directive 2010/75/EU (Integrated Pollution Prevention and Control), pp. 38-54.

[7] Cembureau (1999). Best Available Techniques for the cement industry, pp. 1-12.

[8] Kawatra, S. (2006). Advances in Comminution. Society for Mining, Metallurgy and Exploration Incorporation Publication, Littleton, Colorado USA, pp. 2-150.

[9] Oyepata S. J. and Osawaru T. O. (2022). The Impact of Fossil fuels and Agricultural Wastes Used as Energy Mix on Cement Production: Using Particle Swarm Optimization model. Journal of Energy Technology and Environment, Vol. 4(4): pp. 12-20.

[10] Joseph SO (2018). Optimizing Cost of Production of Cement with Alternative Fuel Mix. Lambert Academic Publication, Chisinau, Republic of Moldova pp. 1-152.

[11] Kumar SD; Kumar JB and Mahesh MH. (2018). Quantum Nanostructures (QDs), pp. 58 – 88.

[12] Peter *del* Strother (2019). Lea's Chemistry of Cement and Concrete, 5th Edition, pp. 2-34.

[13] Aumund Group (2020). Clinker Storage Systems. Technical data, pp. 1-12.

[14] Ileane M; Nicoleta V; George S and Roxana F (2010). Influence of conditions and period of storage for clinker and granulated furnace slag on cement characteristics. Revista Romana de Materiale, 40(2): pp.91-101.

[15] Holderbank (2000b). Process Technology, Mill Ventilation and Cement Cooling Holderbank Financière Glaris Ltd Publication, Glaris Germany, p. 1-35.

[16] Yunus AC (2008). Introduction to Thermodynamics and Heat Transfer, 2nd Edition, McGraw- Hill, pp. 38-89.

[17] John HL and John H (2001). A Heat Transfer Textbook. Published by J. H. Lienhard V, Cambridge Massachusette, 3rd Edition, pp. 20 -35.

[18] Hamed R.T.; Brit A; A. Iman; Zahiruddin F and Abu H (2020). Investigation Thermal Properties of Normal Weight Concrete for Different Strength class. Journal of Environmental Treatment Techniques, vol. 3. No. 3, pp. 908-914.

[19] Iman A; Payam S; Zahiruddin F; Abu H and Norhayati B (2018). Thermal conductivity of concrete. A review, Journal of Building Engineering, vol. 20, pp. 81-93, 52-7102.